Journal of Magnetism and Magnetic Materials 387 (2015) 90–95

Contents lists available at ScienceDirect

Journal of Magnetism and Magnetic Materials

journal homepage: www.elsevier.com/locate/jmmm

Ultrafine grained high density manganese zinc ferrite produced using polyol process assisted by Spark Plasma Sintering

T. Gaudisson [a], Z. Beji [a], F. Herbst [a], S. Nowak [a], S. Ammar [a,*], R. Valenzuela [b]

[a] ITODYS, Université Paris Diderot, Sorbonne Paris Cité, CNRS UMR-7086, 75205 Paris, France
[b] D2MC, Instituto de Investigaciones en Materiales, Universidad Nacional Autónoma de México, 04510 Ciudad de Mexico, Mexico

ARTICLE INFO

Article history:
Received 7 June 2014
Received in revised form
7 March 2015
Accepted 12 March 2015
Available online 18 March 2015

Keywords:
Mn–Zn ferrite spinel
Polyol process
Spark Plasma Sintering
Magnetic single domain grains.

ABSTRACT

We report the synthesis of Mn–Zn ferrite (MZFO) nanoparticles (NPs) by the polyol process and their consolidation by Spark Plasma Sintering (SPS) technique at relatively low temperature and short time, namely 500 °C for 10 min. NPs were obtained as perfectly epitaxied aggregated nanoclusters forming a kind of spherical pseudo-single-crystals of about 40 nm in size. The results on NPs consolidation by SPS underlined the importance of this clustering on the grain growth mechanism. Grain growth proceeds by coalescing nanocrystalline aggregates into single grain of almost the same average size, thus leading to a high density ceramic. Due to magnetic exchange interactions between grains, the produced ceramic does not exhibit thermal relaxation whereas their precursor polyol-made NPs are superparamagnetic.

1. Introduction

Manganese–zinc ferrite oxides (MZFO) play an important role in ferrimagnetic materials because of their remarkable magnetic properties. Indeed, their physical flexibility, high magnetic polarization in combination with a high electrical resistivity, mechanical hardness and chemical stability make them particularly useful for different applications in various electromagnetic fields, ranging from magnetic sensors, microwave absorbers to magnetic reading heads, among others [1]. One of the most important interests for these materials is their ability to be used as high-permeability materials for low-power losses application at relatively high frequencies (~1 MHz) [2,3]. In this case, the technical performances of the produced ferrites are strongly dependent to their microstructure. Indeed, as bulk materials, most of the research related to MZFO ceramics is focused on grain-boundary engineering, since the magnetization reversal in such materials is exclusively driven by domain wall motions. The grain boundaries may represent obstacles to domain movement leading to permeability decrease and power losses increase. Obviously, considerable material engineering effort have been devoted to produce coarse grained MZFO, discarding automatically the processes adapted to fine grained ceramics. As a consequence, the question of the ability of nanostructured ceramics to be used as high permeability materials or power materials when their grain size is lower than the critical diameter associated to transition from a magnetic polydomain configuration to a single domain one remains open, while the solid state physics rules change at these dimensions, introducing another magnetization reversal mechanism, namely, coherent spins rotation. Indeed, it is commonly accepted that when the particle or grain size is reduced to a few of nanometers, the saturation magnetization decreases and the coercive field increases. The enhancement of the randomly canted surface or interface spin fraction contributes to the total magnetization decrease and surface magnetic anisotropy increases [4]. Moreover, the reversal magnetization mechanism changes from a wall displacement driven one (magnetic poly-domains) to a coherent full spins rotation monitored one (magnetic single domain), affecting drastically the dynamic magnetic behavior of the considered materials.

In MZFO, the critical grain size D_{cr} below which the grains become magnetic single domains was first measured to be about 4 μm by neutron depolarization measurements [5]. These measurements showed also that ceramics with grains slightly smaller than 4 μm exhibited a substantial lowering of their energy dissipation in the MHz frequency range [6]. Parallel to that, theoretical calculations based on correction for the soft magnetic environment using magnetostatic calculations, the modified lower and upper bound of the Brown's expression for the critical grain size, yielded values for which the observed value was found to be in between these corrected lower and upper bound [7]. Latter, Aharoni et al. did further micromagnetic calculations to deal with the soft magnetic environment [8]. Finally, Aarts et al. studied the

* Correspondence to: Bâtiment Lavoisier, 15 rue Jean-Antoine de Baïf, 75205 Paris, France. Fax: +33 1 5727 7263.
E-mail address: ammarmer@univ-paris-diderot.fr (S. Ammar).

http://dx.doi.org/10.1016/j.jmmm.2015.03.045
0304-8853/

magnetic domain transition in MnZn-ferrites by Magnetic Force Microscopy (MFM) [9] and confirmed the critical size range. If one excepts these physical studies, experimental data on ultrafine grained MZFO ceramics are rare.

To the best of our knowledge, most of the studied fine grained ceramics were obtained by consolidation of nanoparticles (NPs), using mainly Hot Isostatic Pressing (HIP) [10] and Spark Plasma Sintering (SPS) [11,12] with an average grain size ranging between some micrometers to some submicrometers. MZFO ceramics of less than 100 nm grain size, approaching the smallest possible grain sizes to investigate the magnetic behavior of soft magnets in their true single domain regime, have not been reported. For such a purpose, we prepared MZFO NPs using the polyol process and we used them as starting material to produce nanostructured dense ceramic with grains as fine as possible by means of SPS. We report here measurements of the static magnetic properties of obtained ceramics.

2. Experimental techniques

2.1. Materials processing

2.1.1. Chemicals

$Mn(CH_3CO_2)_2 \cdot 4H_2O$, $Zn(CH_3CO_2)_2 \cdot 2H_2O$, $Na(CH_3CO_2)$ and $FeCl_3$ salts as precursors and ethyleneglycol (hereafter abbreviated as EG) as solvents were purchased from SIGMA-ALDRICH and ACROS Organics, respectively. All reagents were used as received without further purification.

2.1.2. NPs synthesis

MZFO particles were prepared by forced hydrolysis in ethyleneglycol of Manganese, zinc and iron salts in the desired atomic ratio. The total iron concentration was fixed to 0.2 M. Sodium acetate was also added to the mixture in an optimized amount (0.6 M) as well distilled water. The hydrolysis ratio defined as the nominal water to metal molar ratio, was fixed to $h=9$ (optimized value). All the salts were introduced simultaneously in a given volume of EG solvent, and heated (6 °C/min) up to reflux while stirring. The reaction medium was maintained under reflux (~165 °C) for twelve hours. After cooling to room temperature, the solids were separated from the supernatant by centrifugation and washed with ethanol. The powders were then dried in air at 50 °C.

2.1.3. NPs consolidation

The recovered powders (typically 1 g per batch) were introduced into an Ø 8 mm graphite die with a layer of protective papyex. The die is enclosed by graphite punches at both sides which will serve to the uniaxial pressure transmission and DC current pulses delivery in the SPS furnace (DR. SINTER515S SYNTEX SPS). The temperature was then raised relatively slowly (26 °C/min) up to a first plateau of 280 °C (10 min) for outgassing and then rapidly (80 °C/min) to a second one at 500 °C (5 min) for sintering. The pressure was first increased from 0 to 50 MPa at 25 °C, from 50 to 80 MPa at 280 °C and then maintained at 80 MPa up to the end of the operations. The derivative of the distance between crucible pistons, dZ/dt versus time as well as the temperature versus time were simultaneously plotted (Fig. 1) to follow the main changes in the microstructural properties of the starting powder. We assume that when the displacement of punches slows down (dZ/dt is associated with volume contraction at the origin of the MZFO consolidation at constant pressure) the temperature of sintering is reached.

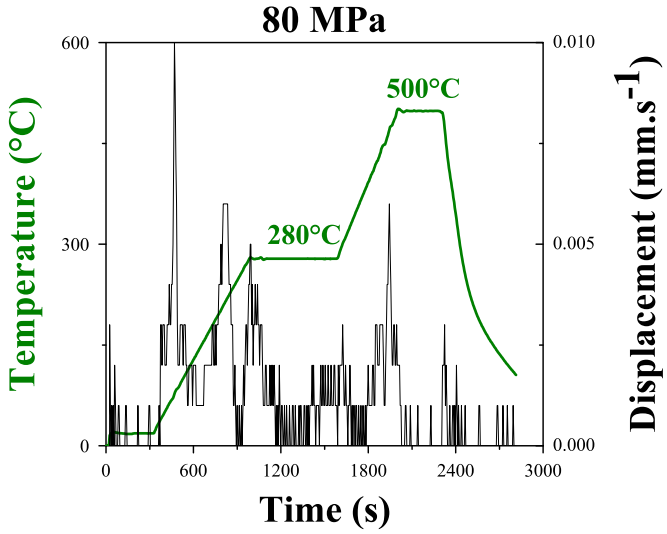

Fig. 1. Typical shrinkage curve and load applied as a function of the sample temperature and shrinkage curve as a function of sintering time in the SPS process of reactivity of MZFO consolidation.

2.2. Material characterization

2.2.1. Phase analysis

To check the exact chemical composition of the produced samples, Inductively Coupled Plasma Atomic Emission Spectroscopy (ICP-AES) and Energy Dispersive spectrometry (EDS) were carried out. ICP-AES was performed at the *Centre d'Analyse de Vernaison*, the French CNRS analysis facility, while EDS was performed using a lab spectrometer mounted on a JEOL-JSM 6100 scanning electron microscope (SEM) operating at 30 kV. The structure of the samples was investigated by X-ray diffraction (XRD) using an Empyrean PANALYTICAL diffractometer equipped with a copper X-ray tube and a 2D PIXCEL detector and a D5000 BRUKER diffractometer equipped with an iron X-ray tube and a punctual scintillating detector. All the XRD patterns were recorded in the Bragg–Brentano θ–θ geometry in the 10–100° 2θ range with a step of 0.01°. The Cell parameters were refined using standard Rietveld program [13]. Crystallite size was calculated from the diffraction line broadening analysis based on the Williamson–Hall method [14], assuming a Lorentzian peak profile and using polycrystalline silicon as standard.

2.2.2. Microstructure analysis

The produced powder was observed by Transmission Electron Microscopy (TEM), using a JEOL-100-CX II TEM microscope working at 100 kV, while the prepared ceramic was observed by Scanning Electron Microscopy (SEM) using a ZEISS Supra 40 FEG-SEM microscope working at 5 kV. The particle and grain size distribution were obtained from the recorded micrographs using SAISAM software (Microvision Instruments), calculating the surface-average diameter of about 200 particles or grains.

2.2.3. Magnetic properties

The variation of the magnetization as a function of temperature and field were carried out using a MPMS-XL Quantum Design SQUID magnetometer. The samples were ground and slightly compacted in a diamagnetic plastic tube.